ChemComm
Chemical Communications

Accepted Manuscript

This article can be cited before page numbers have been issued, to do this please use: K. J. Andersen, A. Asghari Alamdari, A. Smolska, N. Lock, A. Bentien and J. Quinson, *Chem. Commun.*, 2026, DOI: 10.1039/D6CC01485B.

ROYAL SOCIETY OF CHEMISTRY

rsc.li/chemcomm

ChemComm

View Article Online
DOI: 10.1039/D6CC01485B

COMMUNICATION

Surfactant-free $NaBH_4$-mediated synthesis of Au_xPd_{1-x} nano-alloys for active electrocatalysts

Kristian Junker Andersen,[a] Armin Asghari Alamdari,[a] Aleksandra Smolska,[a] Nina Lock,[a] Anders Bentien[a] and Jonathan Quinson*[b,a]

Received 00th January 20xx,
Accepted 00th January 20xx

DOI: 10.1039/x0xx00000x

Nanomaterials with composition Au_xPd_{1-x} (x=0-1) in the size range 5-15 nm are easily obtained at room temperature using a surfactant-free $NaBH_4$-mediated synthesis in water. The materials are readily active electrocatalysts suitable to timely study composition effects, as exemplified with the electrocatalytic ethanol oxidation reaction (EOR).

Nanomaterials (NMs) are relevant for a range of applications and in particular for catalysis due to their size-, structure-, and/or composition- dependent properties.[1] A range of methods have been reported to prepare such nanoparticles (NPs) with a large surface/volume ratio especially relevant for catalysis.[2]

In particular, colloidal syntheses are tractable synthetic approaches, where typically a (metal) precursor in an oxidized state is reduced in the liquid phase.[1, 3] Unfortunately, in most colloidal syntheses, additives or surfactants are used to ensure colloidal stability.[1, 4] Those molecules typically bind to the NP surface, which prevent in most cases the full use of colloidal NPs for catalytic applications. Surfactant-removal can be an option to address this challenge,[5] but it implies processes typically partially successful and/or requiring energy-intensive steps.[1]

To make the most of the versatility of colloidal syntheses[6] but by-pass the challenge of potentially blocked active sites, so-called surfactant-free colloidal syntheses are promising. Those syntheses are defined elsewhere and are relying mainly on electrostatic stabilization.[1, 7] In particular, surfactant-free colloidal syntheses obtained at room temperature in aqueous media using simple chemicals are attractive for safer operation and potentially higher throughput, but also to provide a simple way to prepare NMs that is applicable for non-experts.[1, 3, 7, 8]

Among reported options, Au NPs are easily obtained at room temperature in water without the need for any additives using solely $HAuCl_4$ as precursor and $NaBH_4$ as reducing agent.[9, 10] A similar approach proved to be successful for the preparation of unsupported Pt,[11] Ru[12] and Pd[13] NMs, among other metals,[14] as detailed in Supporting Information (SI). The NPs are promising candidates for catalysis, see **Tab. S1**.[9, 11, 12, 15] For instance, surfactant-free Au NPs obtained by the $NaBH_4$-mediated synthesis are readily active electrocatalysts for the ethanol oxidation reaction (EOR).[16] The EOR is relevant for energy conversion and at the core of direct alcohol fuel cells.[17-19]

However, exploiting this synthesis approach for the timely study of more complex compositions is seldom explored. To the best of our knowledge, only Au_xAg_{1-x} bimetallic NPs have been reported by this approach.[20] The NPs were considered for the 4-nitrophenol reduction as model system for water treatment.

Here, we investigate if other bimetallic nanomaterials than Au_xAg_{1-x} can be obtained to expand the generality and relevance of the synthesis approach. We exploit the fast and simple surfactant-free $NaBH_4$-mediated synthesis method to prepare Au_xPd_{1-x} NPs for electrocatalysis with the example of the EOR. It is well established that Pd is an efficient catalyst for the EOR with relatively poor stability and prone to poisoning, whereas Au is less active but more stable.[8, 21] The rationale to develop Au-Pd materials is also motivated here by the fact that Au[9, 10] and Pd[13] nanomaterials can be obtained by the proposed method. Au is expected to provide stability whereas Pd provides activity for the EOR in alkaline media. In this sense, developing Au_xPd_{1-x} NPs is a promising and common strategy for the EOR[22, 23] and other reactions.[24, 25]

A first finding is that the surfactant-free $NaBH_4$-mediated synthesis leads to NPs in seconds for the whole range of composition from Au only to Pd only, as illustrated in **Fig. 1** and **Fig. S1**. In the present study, a total concentration of metal (Au+Pd) of 0.5 mM and a $NaBH_4$/(Au+Pd) molar ratio of 5 were used. While the as-prepared Au colloids are stable for months, the stability decreases as the Pd content increases, in analogy to what was observed with Au_xAg_{1-x} with an increasing amount of Ag,[20] and in agreement with the relatively lower stability of Pd colloidal materials prepared by the surfactant-free $NaBH_4$-mediated synthesis.[15]

Au-rich dispersions tend to exhibit a red colour whereas Pd-rich dispersions tend to be darker. The plasmonic properties assessed from UV-vis, marked by a pronounced surface plasmon resonance (spr) around 518 nm for Au NPs, are less

[a] Biological and Chemical Engineering Department, Aarhus University, 40 Åbogade, 8200, Aarhus, Denmark
[b] CICA-Centro Interdisciplinar de Química e Bioloxía, Facultade de Ciencias, Universidade da Coruña, Campus de Elviña, A Coruña, Spain
j.quinson@udc.es

† Footnotes relating to the title and/or authors should appear here.

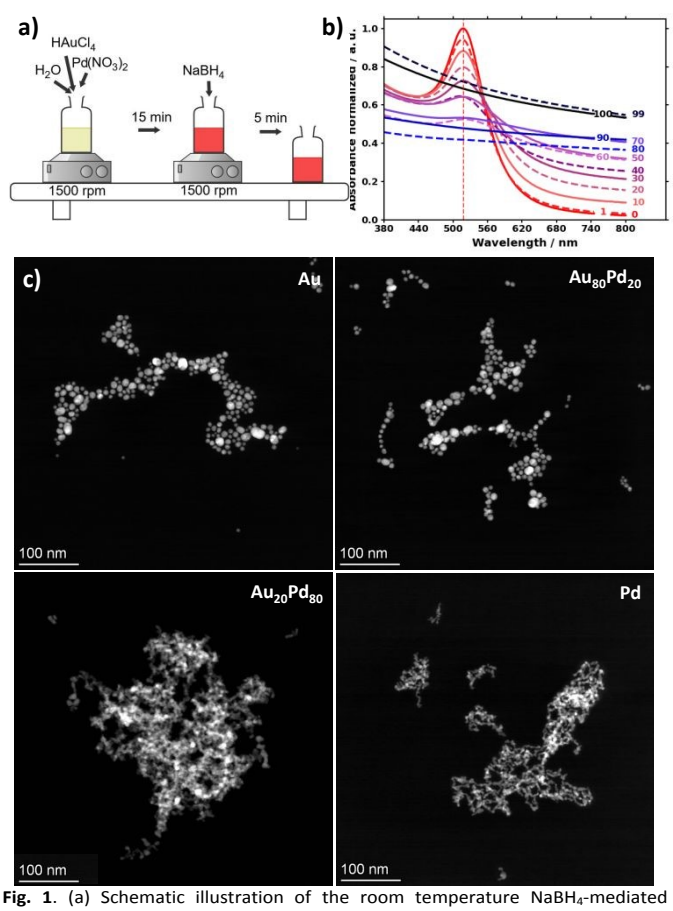

Fig. 1. (a) Schematic illustration of the room temperature $NaBH_4$-mediated surfactant-free synthesis of Au_xPd_{1-x} nanomaterials in water. Retrieved from https://chemix.org and adapted. (b) UV-vis characterization of the resulting materials, the nominal at.% for Pd is indicated. (c) Illustrative STEM micrographs for samples prepared with Au (only), 20 at.% Pd ($Au_{80}Pd_{20}$), 80 at.% Pd ($Au_{20}Pd_{80}$), Pd (only), as indicated.

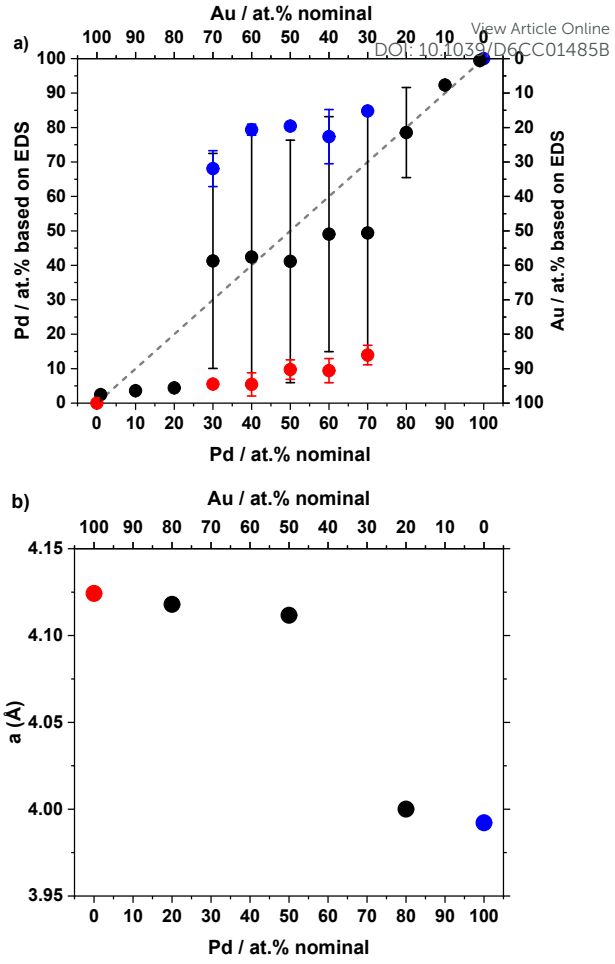

Fig. 2. (a) Experimental composition retrieved from STEM-EDS as a function of nominal composition. For the samples showing two types of nanostructures, the composition retrieved for the Au-rich population is indicated in red and the Pd-rich nanomaterials have a composition indicated in blue. (b) Lattice parameter as a function of nominal composition. See also Fig. S5.

pronounced as the Pd content increases, as it can be expected,[8] see **Fig. S2**.

The size/shape of the NPs evaluated by STEM change from spherical to network-like structure when the amount of Pd increases, which might account for the decreasing colloidal stability, see **Fig. 1**, **Fig. S3** and **Tab. S2**. The average size of the nanomaterials is in the overall range of 5 to 15 nm.

UV-vis, STEM and EDS confirm that the composition and the size can be tuned in the all composition range by adjusting the ratio of the precursors, see **Fig. 1c** and **Fig. 2**. The discrepancy between nominal and experimental composition retrieved from EDS reported in **Fig. 2a** is commonly observed and attributed to experimental errors in the preparation of the stock solutions of metal precursors and/or quantification of the Au and Pd contents. Indeed, STEM-EDS only consider relatively few NPs. A mismatch between nominal and final composition was also observed for Au_xPd_{1-x} materials prepared by a different route,[8] and is also reported for Au_xAg_{1-x}.[20]

It is also interesting to note that the sample with a nominal Pd content of 30 at.% up to 80 at.% Pd tend to show two populations of materials with some Au-rich and some Pd-rich structures, as detailed in **Fig. S4** and reported in **Fig.2a**. Within a same sample, the Au-rich structure tend to be spherical whereas the Pd-rich structure tend to have a more network-like Structure, see **Fig. 1c**. The Au-rich materials tend to be larger than the Pd-rich materials, see **Fig. S3**.

XRD analysis reveals diffraction patterns moving from the typical fcc structure of Au to the fcc structure of Pd with a shift in the lattice parameter from ca. 4.12 Å (Au) to 4.00 Å (Pd) as the Pd amount increases, as detailed in **Fig. 2b**, **Fig. S5** and **Tab. S2**. The Au-rich NPs tend to be larger, see **Fig. S3**, and might dominate the volume-weighted XRD pattern, e.g. in the $Au_{50}Pd_{50}$ sample, which accounts for the trend observed in **Fig. 2b**.

Note that here there is no independent control over size, composition and shape at this stage. Independent control over those interlinked properties could be desirable to disentangle those various effects in catalysis. In this direction, the $NaBH_4$/Au molar ratio was kept to 5 in the present study to minimize the amount of relatively harmful $NaBH_4$ used and because it was shown to lead to the smallest Au NPs in previous studies.[16, 26] It is expected that increasing the $NaBH_4$/Au molar ratio and/or increasing the metal concentration or finer control on the pH will lead to larger NPs, by analogy with what is observed with Au and Au_xAg_{1-x} NPs in previous reports.[20, 27]

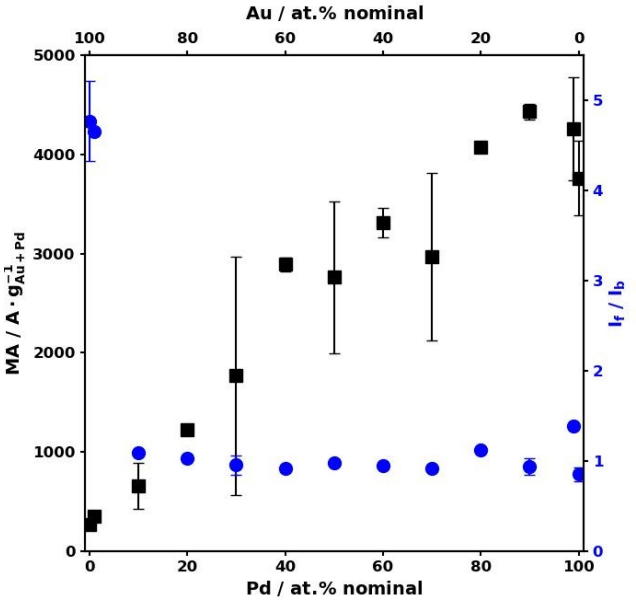

Fig. 3. MA (left-hand side Y-axis black, ■) and I_f/I_b ratio (right-hand side Y-axis, blue, ●) as a function of the sample nominal composition.

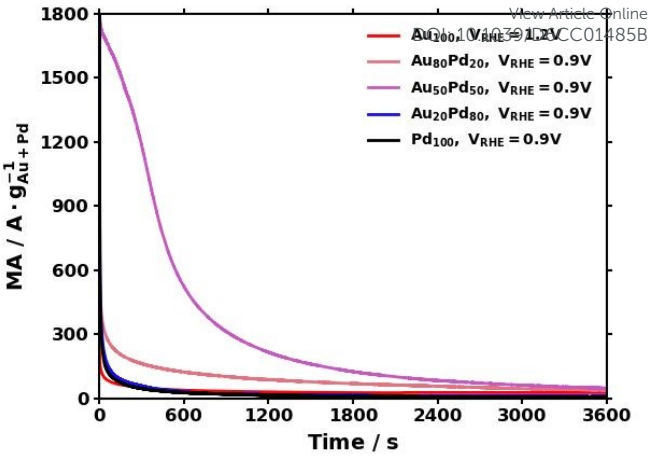

Fig. 4. CA in 1 M KOH + 1 M Ethanol at 1.2 V_{RHE} for the Au sample and 0.9 V_{RHE} for various other samples, as indicated,.

Table 1. MA maintained over time during CA performed for 1 hour at 0.9 V_{RHE} * in 1 M KOH with 1 M Ethanol and before-after CA (assessed by CV).

Sample	MA maintained % (CA) **	MA maintained % (CV) ***	# CV cycles before and after CA	V_{RHE} for CA
Au*	11.3	109.7	5	1.2
$Au_{80}Pd_{20}$	5.2	104.5	25	0.9
$Au_{50}Pd_{50}$	2.6	100.9	15	0.9
$Au_{20}Pd_{80}$	0.6	121.4	10	0.9
Pd	0.1	106.0	5	0.9

* CA performed for 1 hour at 1.2 V_{RHE} for the Au sample
** compared to the activity recorded after 1 s of CA
*** based on CV before and after CA. The number of CVs before CA was chosen to reach a steady MA and this same number of CVs was performed after CA for comparison. The number of CVs is indicated in the last column.

A second finding is that the NPs are readily electrochemically active and therefore can be directly used to assess the EOR activity. See details on the typical data and metrics for this reaction in **SI**, **Figs. S6-S11**. The mass activity (MA, normalized to the nominal metal content) decreases as the Au content increases, see **Fig. 3**. The poisoning resistance tends to increase as the Au content increases, as observed with an overall increase of the I_f/I_b ratio, defined and detailed in SI.[28]

The values obtained in terms of MA and poisoning resistance are promisingly high compared to the literature in particular for Au-Pd materials,[19, 28] as discussed further below.

It is expected that the nanocatalyst stability under electrochemical testing decreases with the Pd content while the overpotential to observe a catalytic behaviour decreases as the amount of Pd increases.[8] Given the potential benefits of Au NPs and Au-rich Au-Pd nanomaterials in terms of stability,[22, 23] a more specific focus is here given to the $Au_{50}Pd_{50}$ and $Au_{80}Pd_{20}$ as illustrative examples, compared to Au only, Pd only and $Au_{20}Pd_{80}$.

Chronoamperometry (CA) was performed at 0.9 V_{RHE} for Pd, $Au_{20}Pd_{80}$, $Au_{50}Pd_{50}$, $Au_{80}Pd_{20}$, and 1.2 V_{RHE} for Au, see **Fig. 4**, see details in **SI** and **Fig. S11**. The higher voltage needed for the Au comes from the higher voltage at which catalysis is observed. The CA leads to a pronounced loss in MA tabulated in **Tab. 1**. As the amount of Au decreases the MA retained decreases and hardly less than 1% of the original MA maintained after 1 hour for the Pd-rich samples, whereas Au-rich samples retain up to 5-10% of activity. Although the MA of the Pd-rich sample is expected to be higher as the Pd content increases, see **Fig. 4**, the relatively low current observed for the Pd only sample illustrates the likely formation of oxidized Pd that it not catalytically active.[29] In particular the $Au_{50}Pd_{50}$ sample shows initially high activity but a loss of MA of more than 99% for 1 hour CA. In contrast, a Au-rich sample such as $Au_{80}Pd_{20}$ show a relatively low MA but maintain a relatively higher activity over time (loss of 95% based on CA).

After CA, performing several CVs re-activate the materials, as illustrated in **Tab. 1** and **Fig. S11**. Those results suggest that leaching is not the main mechanism of activity loss over time and that further optimization of the electrochemical testing could lead to higher catalytic activity maintained under continuous operation, e.g. by supporting the material.[3, 30]

Finally, it is a general challenge to compare materials synthesized by different methods and with catalytic activity evaluated by different protocols in the literature (different syntheses, sizes, compositions, different setups, NP supported or not on other materials, different concentrations and nature of electrolytes, different potential ranges, different normalization, etc.).[3, 19, 31, 32] Nevertheless, the materials obtained here are relatively more active than in other reports. A MA for Au NPs of 250 A g_{Au}^{-1} is higher than for most other reports and comparable to values reported for Au NPs prepared by a surfactant-free ethanol mediated synthesis reported elsewhere.[28, and references therein] A MA for Pd NPs of 4 000 A g_{Pd}^{-1} is higher than most reported giving values closer to 3000 A g_{Pd}^{-1} or lower.[13, 23, 30, 33] Equally the bimetallic material give relatively high MAs (at similar compositions) compared to other Au-Pd materials in the range of 400-3000 A g_{Au+Pd}^{-1},[23, 34] for instance

for materials obtained via a similar approach as the one reported here but with polyvinylpyrrolidone (PVP)[34] or Triton as additives.[35]

The results point towards the benefits of a surfactant-free approach leading to more active NPs and toward Au-rich materials to develop promising catalysts for the EOR. Despite the relative inhomogeneity of the sample with Pd- and Au-rich materials within the same batch, the overall strategies still leads to active materials, probably due to *in situ* further alloying as pointed out elsewhere with nanocomposites,[8] although a full study of such phenomenon is beyond the scope of the present report.

On a final note, surfactant-free colloidal NPs remain relatively scarce compared to their surfactant-assisted counterpart, yet they are promising strategies to develop catalysts[1]. As a consequence, the comparison of colloidal NPs obtained by different surfactant-free strategies are only emerging. In our previous work we showed that Au_xPd_{1-x} NPs could be obtained at room temperature by simply using alkaline ethanol in water as reducing agent.[8] A first benefit of using the milder reducing agent ethanol was that stable colloids were obtained for the all range of composition from Au only to Pd only, as opposed to the present case. Furthermore, spherical NPs were obtained for the all composition range. However the synthesis is much slower than the present $NaBH_4$-mediated approach.

Interestingly, in that previous work,[8] an optimal composition of $Au_{65}Pd_{35}$ was identified to obtain higher MA for the EOR, in agreement with other work,[36] with a value around 2400 A g_{Au+Pd}^{-1}. This was attributed to a balance between a smaller size of the Au_xPd_{1-x} NPs offering a higher surface area leading to a higher MA as the Pd amount increases, and lower stability of the spherical small size Pd-rich NPs obtained. Here, no optimum is observed, see **Fig. 3**. This is attributed to a minor change in size, see **Tab. S2**, but a significant change in shape together with composition (where Pd-rich network like structures are likely more stable than small size spherical NPs for electrocatalysis, although a detailed comparison is beyond the scope of this communication). Furthermore, the NP obtained here for similar composition exhibit a higher MA of ca. 3000 A g_{Au+Pd}^{-1}, highlighting the potential benefits of the surfactant-free $NaBH_4$-mediated synthesis to develop active catalysts.

The results highlights the under-tapped potential of surfactant-free room temperature $NaBH_4$-mediated syntheses of multi-metallic NPs in aqueous media as a simple strategy to obtain composition-controlled nanomaterial directly relevant for electrocatalysis. The synthetic approach could be a key to timely screen larger parameter spaces for NP synthesis and/or catalysis and is relevant to address pending challenges in data driven research.[37] Indeed, the synthesis allows a relatively high throughput due to its simplicity and short reaction time without the need for advanced facilities such as automated stations.

In conclusion, Au_xPd_{1-x} NPs with controlled overall composition are easily obtained at room temperature using a surfactant-free $NaBH_4$ mediated synthesis. The NPs are readily active materials for the EOR. The results show and stress the potential of this approach probably under-exploited to rapidly assess the effect(s) of composition on nano-alloys in (electro)catalysis.

Conceptualization: JQ; Data curation: KJA, AAA, AS; Formal analysis: KJA, AAA, AS; Funding acquisition: JQ, NL, AAA; Investigation: KJA, AAA, AS; Methodology: JQ; Project administration: JQ; Resources: JQ, NL; Supervision: JQ, NL, AB; Validation: KJA; Visualization: KJA, AS; Writing – original draft: JQ, KJA; Writing – review & editing: KJA, AAA, AS, NL, AB, JQ.

JQ, NL and AS thank the Independent Research Fund (DFF) for support via a DFF-Green grant (Light-SCREEN, 3164-00128B). The XRD instrument was supported by the Carlsberg Foundation (Grant no: CF18-0840). JQ thanks the Aarhus University Research Foundation, grant number AUFF-E-2022-9-40. JQ thanks the MCIN/AEI/10.13039/501100011033 and ESF+ for his Ramón y Cajal contract (RYC2023-042920-I). JQ thanks the INTALENT program of UDC and INDITEX. This work was funded by the European Union under the Marie Skłodowska-Curie Postdoctoral Fellowship (Project 101205473 – ZAIRWAYS, AAA). Views and opinions expressed are however those of the authors only and do not necessarily reflect those of the European Union or the European Research Executive Agency. Neither the European Union nor the granting authority can be held responsible for them. Funding for open access charge: Universidade da Coruña/CISUG.

Data availability

The data supporting this article have been included as part of the supplementary information (SI). Supplementary information: additional literature, materials and methods, characterization by XRD, STEM-EDS, UV-vis spectroscopy and electrochemical methods in .pdf format.

Conflicts of interest

There are no conflicts to declare

Notes and references

1. J. Quinson, S. Kunz and M. Arenz, *ACS Catalysis*, 2023, **13**, 4903–4937.
2. C. D. De Souza, B. R. Nogueira and M. Rostelato, *Journal of Alloys and Compounds*, 2019, **798**, 714-740.
3. J. Quinson, S. Kunz and M. Arenz, *ChemCatChem*, 2021, **13**, 1692-1705.
4. L. M. Rossi, J. L. Fiorio, M. A. S. Garcia and C. P. Ferraz, *Dalton Transactions*, 2018, **47**, 5889-5915.
5. M. Cargnello, C. Chen, B. T. Diroll, V. V. T. Doan-Nguyen, R. J. Gorte and C. B. Murray, *Journal of the American Chemical Society*, 2015, **137**, 6906-6911.
6. Y. T. Guntern, V. Okatenko, J. Pankhurst, S. B. Varandili, P. Iyengar, C. Koolen, D. Stoian, J. Vavra and R. Buonsanti, *ACS Catalysis*, 2021, **11**, 1248-1295.
7. S. Reichenberger, G. Marzun, M. Muhler and S. Barcikowski, *ChemCatChem*, 2019, **11**, 4489-4518.
8. J. Quinson, O. Aalling-Frederiksen, W. L. Dacayan, J. D. Bjerregaard, K. D. Jensen, M. R. V. Jørgensen, I. Kantor, D. R. Sørensen, L. Theil Kuhn, M. S. Johnson, M. Escudero-Escribano, S. B. Simonsen and K. M. Ø. Jensen, *Chemistry of Materials*, 2023, **35**, 2173–2190.

9. C. Deraedt, L. Salmon, S. Gatard, R. Ciganda, R. Hernandez, J. Ruiz and D. Astruc, *Chemical Communications*, 2014, **50**, 14194-14196.
10. M. Iqbal, G. Usanase, K. Oulmi, F. Aberkane, T. Bendaikha, H. Fessi, N. Zine, G. Agusti, E. Errachid and A. Elaissari, *Materials Research Bulletin*, 2016, **79**, 97-104.
11. R. P. Charde, B. van Devener and M. M. Nigra, *Catalysts*, 2023, **13**, 248.
12. S. Anantharaj, M. Jayachandran and S. Kundu, *Chemical Science*, 2016, **7**, 3188-3205.
13. A. Ipadeola, B. Salah, A. Ghanem, D. Ahmadaliev, M. Sharaf, A. Abdullah and K. Eid, *Heliyon*, 2023, **9**, e16890.
14. M. Wuithschick, S. Witte, F. Kettemann, K. Rademann and J. Polte, *Physical Chemistry Chemical Physics*, 2015, **17**, 19895-19900.
15. F. Kettemann, M. Wuithschick, G. Caputo, R. Kraehnert, N. Pinna, K. Rademann and J. Polte, *CrystEngComm*, 2015, **17**, 1865-1870.
16. H. K. Fokam, A. Smolska and J. Quinson, *Journal of Materials Chemistry A*, 2026. Accepted. DOI: 10.1039/D5TA08597G.
17. E. Antolini and E. R. Gonzalez, *Journal of Power Sources*, 2010, **195**, 3431-3450.
18. Y. Wang, S. Z. Zou and W. B. Cai, *Catalysts*, 2015, **5**, 1507-1534.
19. L. Yaqoob, T. Noor and N. Iqbal, *RSC Advances*, 2021, **11**, 16768-16804.
20. N. E. Larm, J. A. Thon, Y. Vazmitsel, J. L. Atwood and G. A. Baker, *Nanoscale Advances,* 2019, **1**, 4665-4668.
21. Y. Y. Feng, Z. H. Liu, Y. Xu, P. Wang, W. H. Wang and D. S. Kong, *Journal of Power Sources*, 2013, **232**, 99-105.
22. L. S. R. Silva, C. V. S. Almeida, C. T. Meneses, E. A. Batista, S. F. Santos, K. I. B. Eguiluz and G. R. Salazar-Banda, *Applied Catalysis B-Environmental*, 2019, **251**, 313-325.
23. B. Hanqi, J. Xu, X. Zhu and C. Kan, *Nanoscale Advances*, 2022, **4**, 1827-1834.
24. Y. Zhang, Z. Lyu, Z. Chen, S. Zhu, Y. Shi, R. Chen, M. Xie, Y. Yao, M. Chi, M. Shao and Y. Xia, *Angewandte Chemie-International Edition*, 2021, **60**, 19643-19647.
25. X. Y. Huang, O. Akdim, M. Douthwaite, K. Wang, L. Zhao, R. J. Lewis, S. Pattisson, I. T. Daniel, P. J. Miedziak, G. Shaw, D. J. Morgan, S. M. Althahban, T. E. Davies, Q. He, F. Wang, J. L. Fu, D. Bethell, S. McIntosh, C. J. Kiely and G. J. Hutchings, *Nature*, 2022, **603**, 271-275.
26. K. J. Andersen, M. Varga, A. Smolska, G. Nordhal, J. H. Jensen, R. Moreno, E. D. Bøjesen, A. S. Anker and J. Quinson, *Nano Letters*, 2025, **25**, 15436–15442.
27. J. Quinson, A. Dworzak, S. B. Simonsen, L. T. Kuhn, K. M. O. Jensen, A. Zana, M. Oezaslan, J. J. K. Kirkensgaard and M. Arenz, *Applied Surface Science*, 2021, **549**, 149263.
28. D. Panagopoulos, A. Asghari Alamdari and J. Quinson, *Materials Today Nano*, 2025, **29**, 100600.
29. Z. Liang, T. Zhao, J. Xu and L. Zhu, *Electrochimica Acta*, 2009, **54**, 2203-2208.
30. J. Quinson, S. B. Simonsen, L. T. Kuhn, S. Kunz and M. Arenz, *RSC Advances*, 2018, **8**, 33794-33797.
31. A. R. Zeradjanin, *ChemSusChem*, 2018, 11, 1278-1284.
32. S. Nösberger, J. Du, J. Quinson, E. Berner, A. Zana, G. K. H. Wiberg and M. Arenz, *Electrochemical Science Adances*, 2022, **3**, e2100190.
33. L. Zang, J. Yan, M. Pang, B. Zhang, J. Chen and P. Guo, *Langmuir*, 2021, **37**, 13132-13140.
34. S. Y. Shen, Y. G. Guo, L. X. Luo, F. Li, L. Li, G. H. Wei, J. W. Yin, C. C. Ke and J. L. Zhang, *Journal of Physical Chemistry C*, 2018, **122**, 1604-1611.
35. L. Wang, Z. Liu, S. Zhang, M. Li, Y. Zhang, Z. Li and Z. Tang, *International Journal of Hydrogen Energy*, 2021, **46**, 8549-8556.
36. H. H. Lin, M. Muzzio, K. C. Wei, P. Zhang, J. R. Li, N. Li, Z. Y. Yin, D. Su and S. H. Sun, *ACS Applied Energy Materials*, 2019, **2**, 8701-8706.
37. R. W. Epps and M. Abolhasani, *Applied Physics Reviews*, 2021, **8**, 041316.

View Article Online
DOI: 10.1039/D6CC01485B

The data supporting this article have been included as part of the supplementary information (SI). Supplementary information: additional literature, materials and methods, characterization by XRD, STEM-EDS, UV-vis spectroscopy and electrochemical methods in .pdf format